

DesignCon 2013

Fast, efficient and accurate: via
models that correlate to 20 GHz

Michael Steinberger, SiSoft

Eric Brock, SiSoft

Donald Telian, SiGuys

Abstract

A comparison of modeled to measured results suggests that vias introduce dissipative loss beyond that predicted by modeling tools, especially at frequencies above 10 GHz. This paper presents such a comparison based on measured results from several different test boards using different materials and layout approaches. It evaluates several hypotheses that might explain the additional loss, including leakage from radial TEM waves and interactions with ground vias. The conclusions are used to extend existing analytic via models and improve high frequency behavior. The results of system correlations are presented, demonstrating signal path correlation up to 20 GHz.

Author(s) Biography

Michael Steinberger, Ph.D., Lead Architect for SiSoft, has over 30 years' experience designing very high speed electronic circuits. Dr. Steinberger holds a Ph.D. from the University of Southern California and has been awarded 14 patents. He is currently responsible for the architecture of SiSoft's Quantum Channel Designer tool for high speed serial channel analysis. Before joining SiSoft, Dr. Steinberger led a group at Cray, Inc. performing SerDes design, high speed channel analysis, PCB design and custom RAM design.

Eric Brock, Principal Member of Technical Staff at SiSoft, works closely with customers and semiconductor vendors involved in the design and analysis of multi-GHz serial links. He has analyzed dozens of high-speed parallel and serial interfaces since joining SiSoft in 2002. Prior to SiSoft, he worked at Compaq Computer as a Signal Integrity Engineer in the Alpha Development Group. He received his BS in Electrical Engineering and a BS in Physics from Portland State University in 1998.

Donald Telian is an independent Signal Integrity Consultant. Building on over 25 years of SI experience at Intel, Cadence, HP, and others, his recent focus has been on helping customers correctly implement today's Multi-Gigabit serial links. His numerous published works on this and other topics are available at his website siguys.com. Donald is widely known as the SI designer of the PCI bus and the originator of IBIS modeling and has taught SI techniques to thousands of engineers in more than 15 countries.

1.0 Introduction

This paper reports on a continuing effort to improve electrical channel models at higher frequencies. Previous papers [1-4] reported on improvements that collimated in electrical channel models which accurately reproduced measured data beyond 5 GHz. These models have been well suited for estimating the performance of high speed serial channels up to 6 Gb/s. As the data rate doubles to 12 Gb/s and then more than doubles to 28 Gb/s, however, these models will need to be improved.

Within this modeling effort, via modeling has become increasingly important, and via models have become increasing complex. [1] presented a via model in the form of closed form equations which were derived directly from Maxwell's equations and reproduced measured data extremely well. This model represented the via barrels as multiconductor transmission lines whose characteristic impedances were derived directly from the physical properties of the via. [4] extended the via barrel model to include the printed circuit board pads and entry/exit traces at the ends of the via. Since all of these models represented the via using an equivalent circuit, they have been computationally efficient as well as accurate.

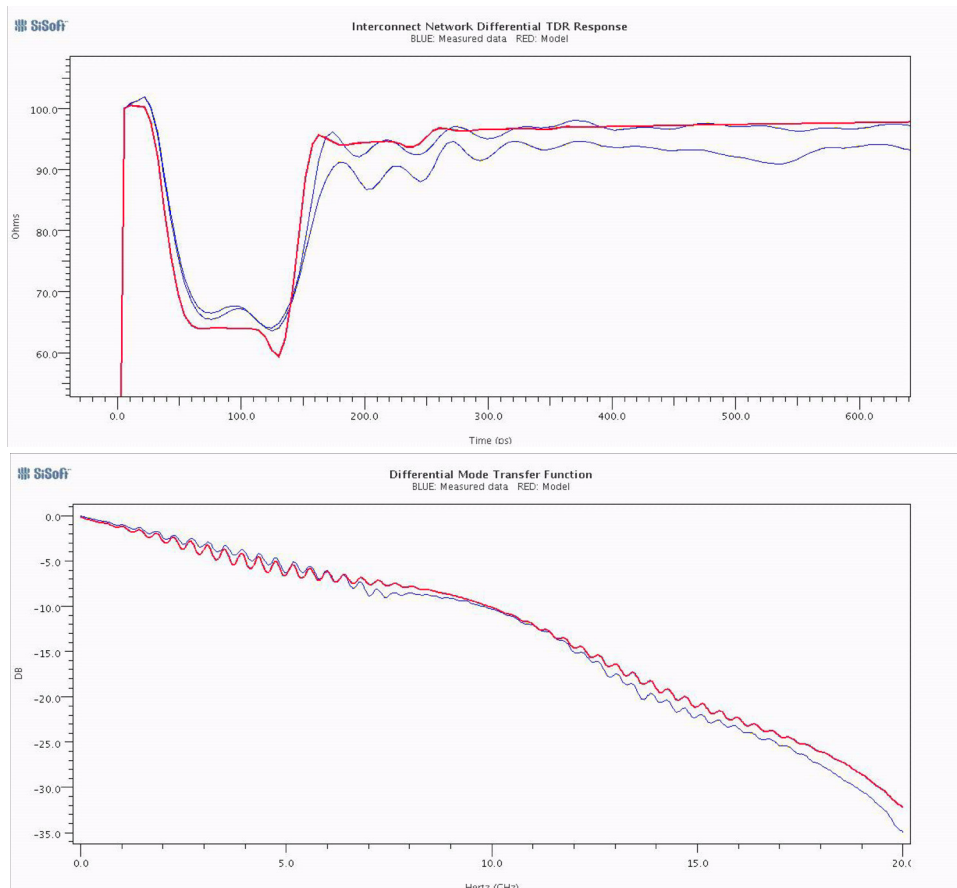


FIGURE 1. Example of model correlation reported in 2012 [4]

Every comparison of model to measurement has compared time domain reflectometry (TDR) waveforms as well as loss vs. frequency curves. The TDR waveforms directly address the accuracy of the impedances in the model and also help to make sure that the elements of the model correspond directly to physical structures. TDR is not, however, a sensitive indicator of transmission loss, and so the loss vs. frequency curves are the other essential element in any model comparison.

Figure 1 is an example of both the TDR and insertion loss model correlation reported in 2012.

To further improve electrical channel models, we approached the problem as an exercise in experimental Physics. That is, we examined the discrepancies between model and measured data across a range of conditions, looked for hypotheses that could explain these discrepancies, tested these hypotheses by empirically modifying the models, and then looked for theoretical explanations for the empirical models. The reference data has always been data measured directly on physical structures, and computational results have always been treated as models. This work continues; however, we believe that what we have learned has engineering value.

When comparing model to measured data, we observed two discrepancies that seemed to be of primary importance:

1. At higher frequencies, the models seem to consistently under-estimate the insertion loss.
2. Whereas the models accurately reproduce the characteristic impedance for longer vias, they consistently predict a lower impedance than was measured for shorter vias.

From the various conversations and meetings we've been involved in, we believe that the first of these two discrepancies, under prediction of insertion loss at higher frequencies, has been widely observed across existing tools, published equations, and correlation attempts published within standards bodies. We do not have any publicly available references that we can refer to, however.

In this paper, we offer two hypotheses to explain the discrepancies stated above:

1. At higher frequencies, vias fail to completely contain their fields, resulting in energy leakage and subsequent dissipation as radial TEM waves between the ground (and virtual ground) planes in the PC board.
In short, vias directly generate a substantial amount of high frequency loss.
2. The transition from between via propagation (perpendicular to the plane of the PC board) to trace propagation (parallel to the plane of the PC board) generates higher order radial TEM waves that introduce a substantial amount of high frequency loss and increase the impedance near the transition.
In short, transitions between vias and traces directly generate a substantial amount of high frequency loss and increase the impedance near the transition.

Furthermore, the theoretical evaluation of these hypotheses suggests that use of racetrack-type antipads should minimize high frequency loss.

2.0 Baseline Data and Model

The baseline for this study was data measured on eight transmission paths with a wide range of trace lengths and via lengths. The device under test was the bare board for a production backplane, and the measurements were made between pads associated with connector pins.

As shown in Figure 2, the circuit model consisted of a differential trace between two vias on a circuit board fabricated using Megtron 6 dielectric. Lossless transmission lines were placed at the input and output to compensate for anticausal numerical artifacts in the TDR calculation [5].

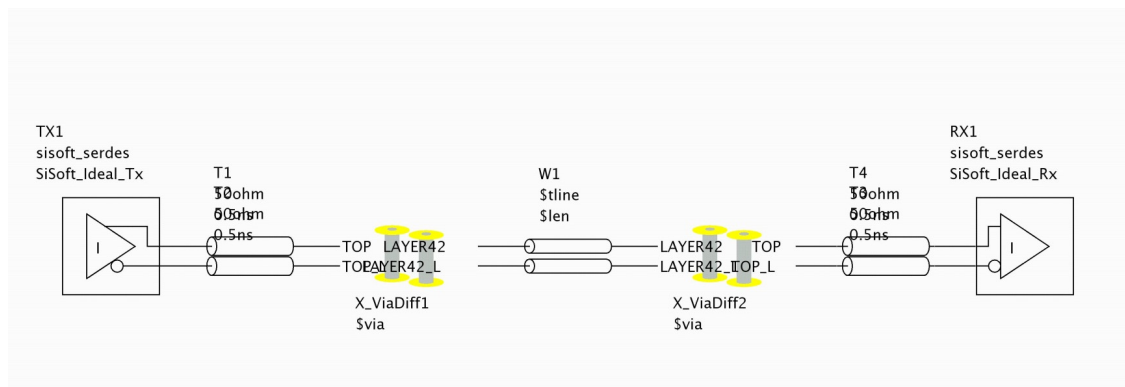


FIGURE 2. Model of baseline configuration

Physical dimensions were taken directly from the circuit board that was measured. Transmission line trace lengths were derived from post-layout extraction of the artwork while dielectric and conductor thicknesses were measured directly from a cross section of the board taken after the electrical measurements were made.

The baseline via model was that described in [4]. It consisted of a top layer pad, a via barrel modeled as a lossless transmission line, a routing layer pad and an exit trace.

The transmission line model was a SPICE RLGC W line model which included closed form equations for the following effects:

- Dielectric loss: Dielectric loss tangent was assumed to be constant with frequency and used the formulation in [6] to model the variation of dielectric constant with frequency.

One set of values was used for the stripline routing layers while a separate set of values was used for a dual stripline layer at the bottom of the board.

TABLE 1. Transmission line dielectric modeling parameters

Parameter	Stripline routing layers	Dual stripline layer	Published range of values
Dielectric constant Dk at 1 GHz	3.55	3.67	3.4 - 3.6
Dielectric loss tangent Df	0.005	0.006	0.004 - 0.006
Differential impedance Z_{00}	90.3 Ω	88.6 Ω	

- Conductor roughness: The conductor roughness model was the one provided in [7]. The conductor roughness value used was 0.15 μrms , which is typical for a circuit board with high quality copper conductors.
- Conductor internal impedance: The modeling of skin effect and the penetration of magnetic fields into the transmission line center conductor are described in [8], which in turn refers to [9], [10], and [11].

To simplify preliminary data analysis, the loss discrepancy was quantified as the difference, in dB, between the modeled loss and the measured loss at 20 GHz.

2.1 Transmission Line Hypothesis

To explain the remaining loss discrepancy, one of the hypotheses we evaluated was the possibility that there were losses in the transmission lines that were not included in the model. We were aware that some EDA tools had implemented models that use tables of dielectric loss tangent vs. frequency, and that some system developers were attempting to use this form of modeling to explain the loss discrepancies. We are still not aware of any published results.

If this hypothesis is correct, then the loss discrepancy should be a linear function of trace length.

Figure 3 is a scatter plot of loss discrepancy at 20 GHz in dB vs. trace length in inches. This scatter plot demonstrates that our measured data does not support the excess trace loss hypothesis, in that short traces seem to have the same range of loss discrepancies as long traces.

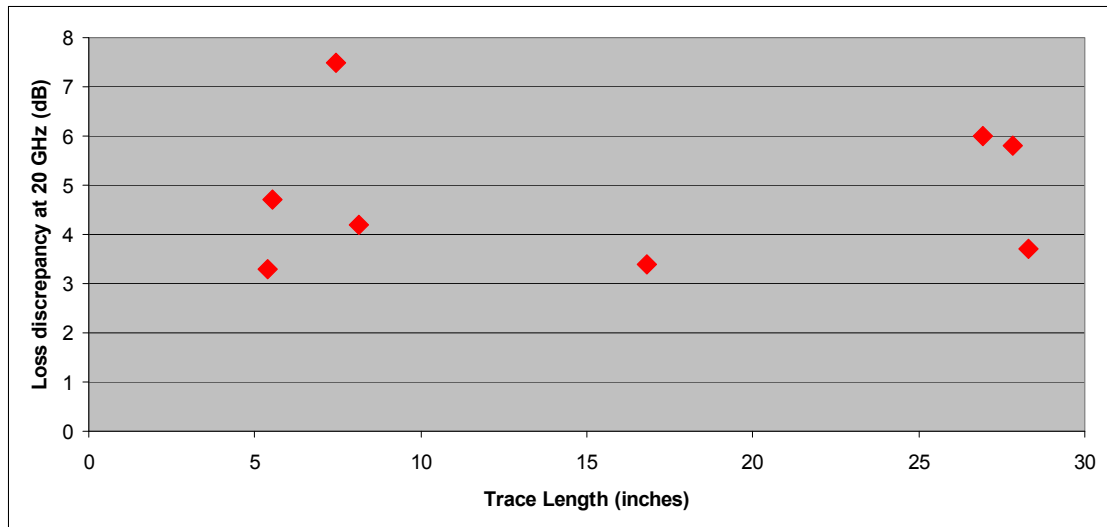


FIGURE 3. Loss discrepancy vs. trace length

We have therefore concluded that our current modeling of transmission line loss is much more accurate than other parts of our model. There is data from materials suppliers that indicates that the dielectric loss tangent can vary by as much as perhaps 20% from 1 GHz to 20 GHz, and we believe that data is accurate and reliable. It appears, however, that one can produce a sufficiently accurate model of transmission line loss by choosing the dielectric loss tangent at a frequency which is approximately half the data rate, and assuming that that dielectric loss tangent applies to all frequencies of interest.

2.2 Via Hypothesis

Since the loss discrepancy appears to be independent of trace length, we looked for some other structure in the measured circuits that might be the location of the excess high frequency loss. Since the only other structures in the measured circuits were vias, we considered the possibility that the excess loss was in the vias. Each measured circuit had two and only two differential vias, independent of trace length; however, the length of the vias varied between the circuits measured, thus providing a means for evaluating this hypothesis.

If the excess loss is in the vias, then the loss discrepancy should be a linear function of via length.

Figure 4 is a scatter plot of loss discrepancy at 20 GHz, in dB, vs. via length in inches. As demonstrated by the dashed line in Figure 4, the measured data suggests that the excess via loss hypothesis is plausible.

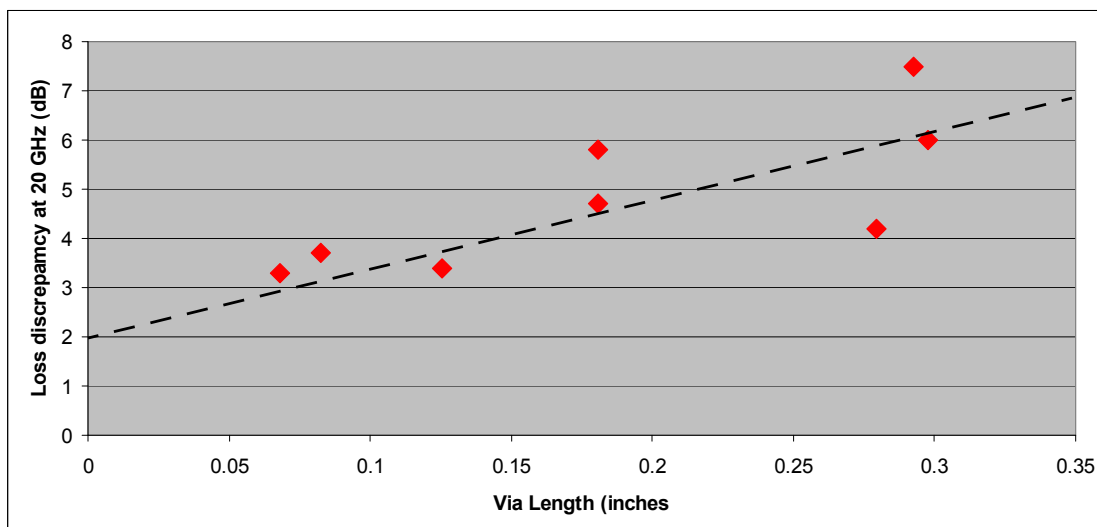


FIGURE 4. Loss discrepancy vs. via length

3.0 Empirical Model of Via Loss

To further evaluate the excess via loss hypothesis, we created an empirical model of via loss. The purpose of this model was to determine whether additional loss in the vias could minimize the discrepancy between modeled and measured insertion loss, and not necessarily to address the Physics associated with any specific loss mechanism.

Since the excess loss appears to be a function of via length, the empirical model adds loss to the via barrel while keeping the pad and exit trace models constant. Furthermore, on the supposition that the excess loss is somehow associated with the series impedance of the ground return path, the empirical model adds resistance to the ground conductor and, to maintain causality, adds an inductive reactance equal to the series resistance.

The resulting excess series impedance per unit length is

$$z(f) = (1 + j)r_v \left(\frac{f}{f_0} \right)^p \quad (\text{EQ 1})$$

This impedance was added to the RLGC W line model of the via barrel. The initial implementation was a stand-alone table driven model and, once the equation was well established, incorporated as an additional frequency dependent component into the W line model in the channel simulator (QCD from SiSoft).

The parameters in Equation 1 were adjusted to optimize the match between modeled and measured loss for the cases described above. We found that the excess loss required for the shorter vias was greater than that for the longer ones. This is consistent with the fact that

the fit line (dotted line) in Figure 4 intercepts the Y axis at a positive value. The values chosen are reported in the following table:

TABLE 2. Empirical model parameters for Equation 1

Via Length	r_v	p	f_0
0.298"	60Ω	3	5.0 GHz
0.293"	60Ω	3	5.0 GHz
0.280"	60Ω	3	5.0 GHz
0.181"	60Ω	3	5.0 GHz
0.125"	60Ω	3	5.0 GHz
0.083"	60Ω	3	3.5 GHz
0.068"	60Ω	3	3.5 GHz

As can be seen in this table, the parameters for all of the via lengths are identical except that the corner frequency shifts from 5.0 GHz to 3.5 GHz for the shortest via lengths. Given that the frequency is taken to the third power, this corresponds to a factor of 2.9 in the excess via loss.

3.1 Comparison to Baseline Data

The following figures compare the measured insertion loss (RED) to the baseline model loss (BLUE) and empirical model insertion loss (YELLOW) for each of the cases in the baseline data set. While the correlation to measured data still isn't perfect, it is very much improved for the empirical model. This tends to confirm the hypothesis that the excess loss is in the vias.

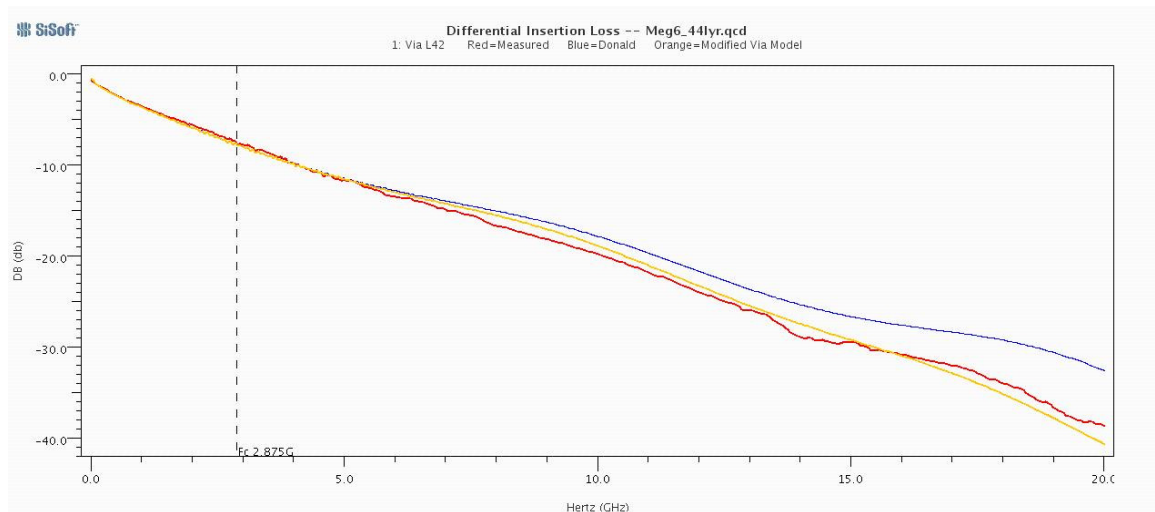


FIGURE 5. Modeled vs. measured insertion loss for 26.9" path length and 0.298" via length

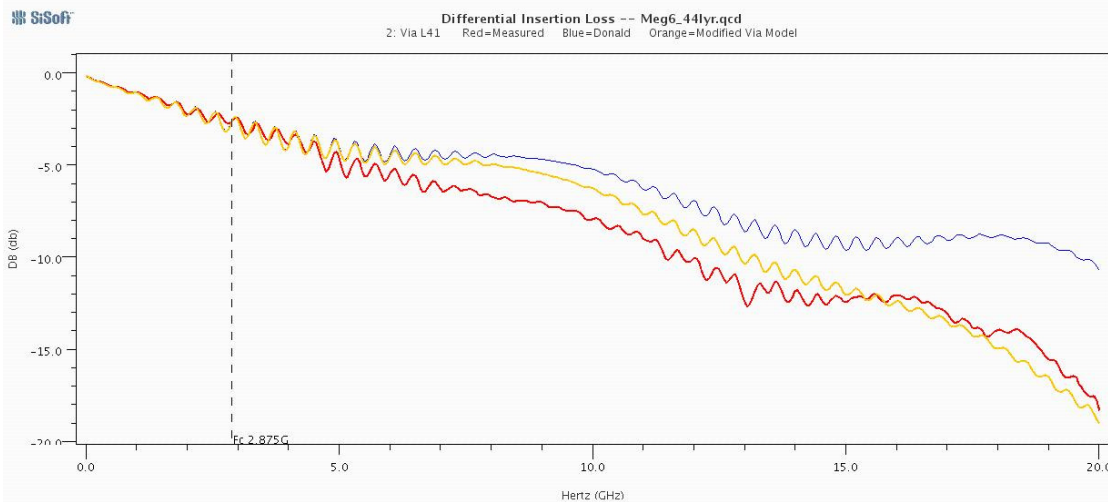


FIGURE 6. Modeled vs. measured insertion loss for 7.5" path length and 0.293" via length

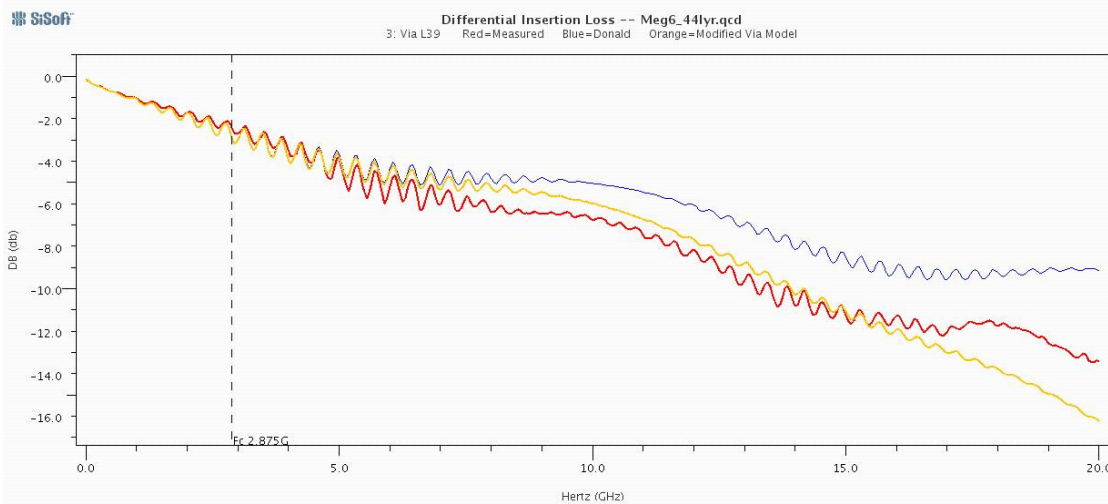


FIGURE 7. Modeled vs. measured insertion loss for 8.0" path length and 0.280" via length

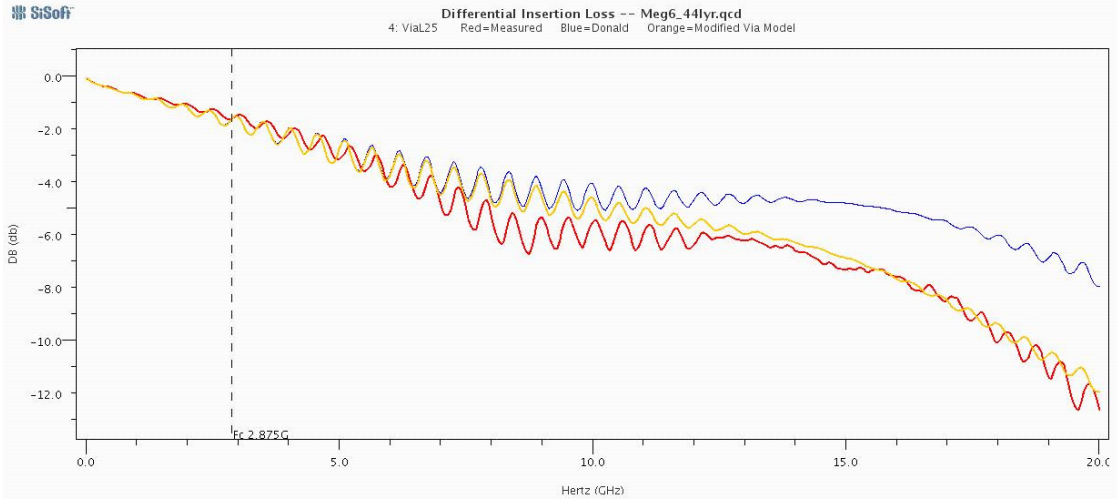


FIGURE 8. Modeled vs. measured insertion loss for 5.5” path length and 0.181” via length

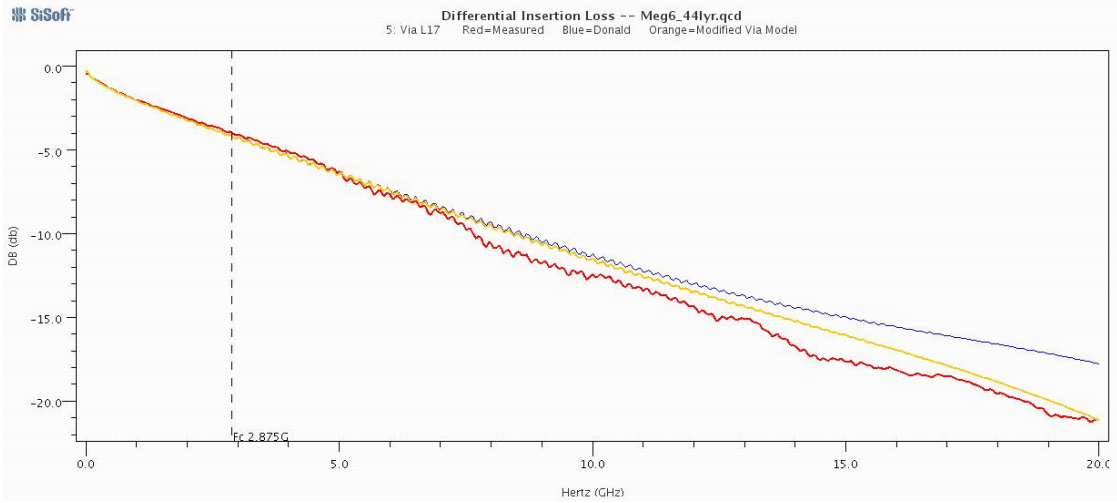


FIGURE 9. Modeled vs. measured insertion loss for 16.8” path length and 0.125” via length

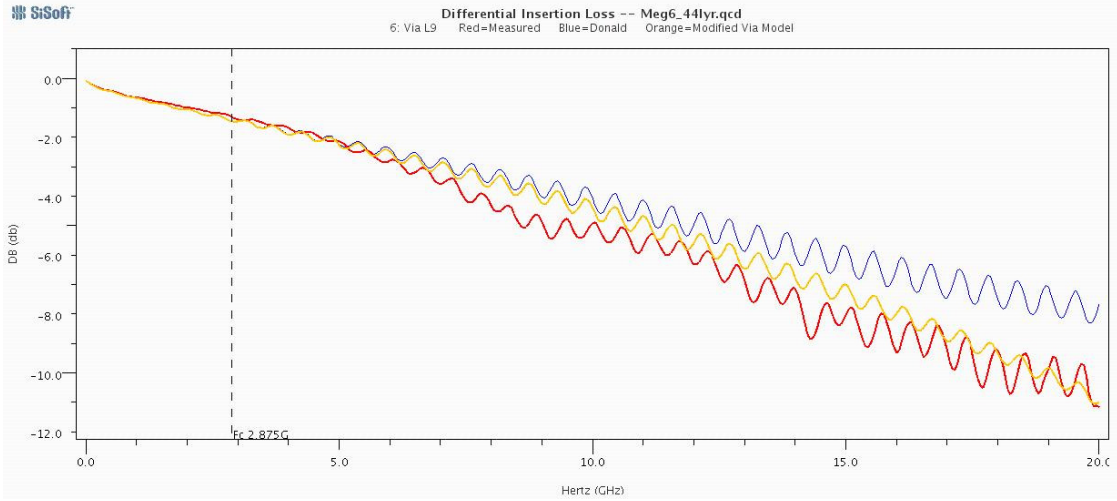


FIGURE 10. Modeled vs. measured insertion loss for 5.4” path length and 0.068” via length

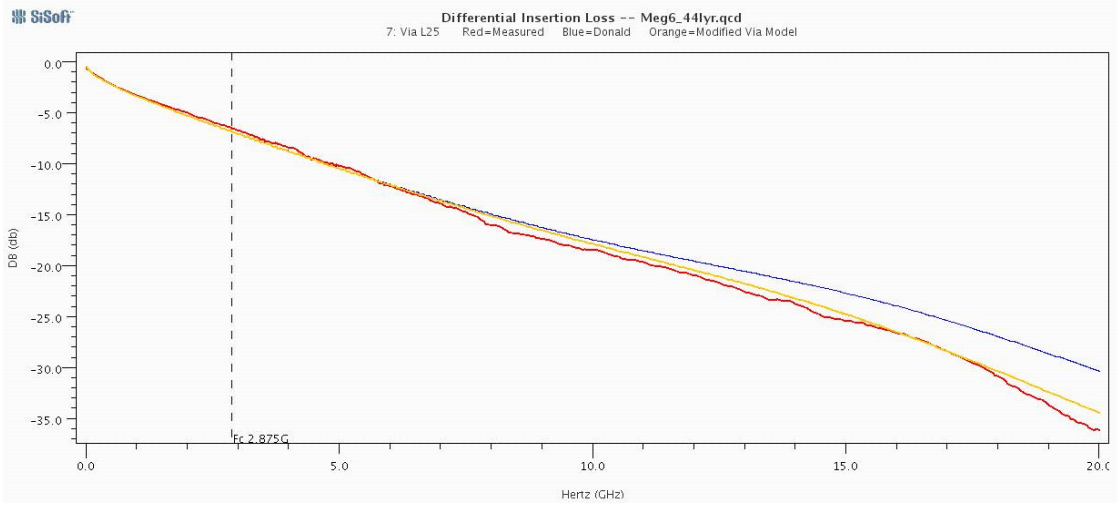


FIGURE 11. Modeled vs. measured insertion loss for 27.6” path length and 0.181” via length

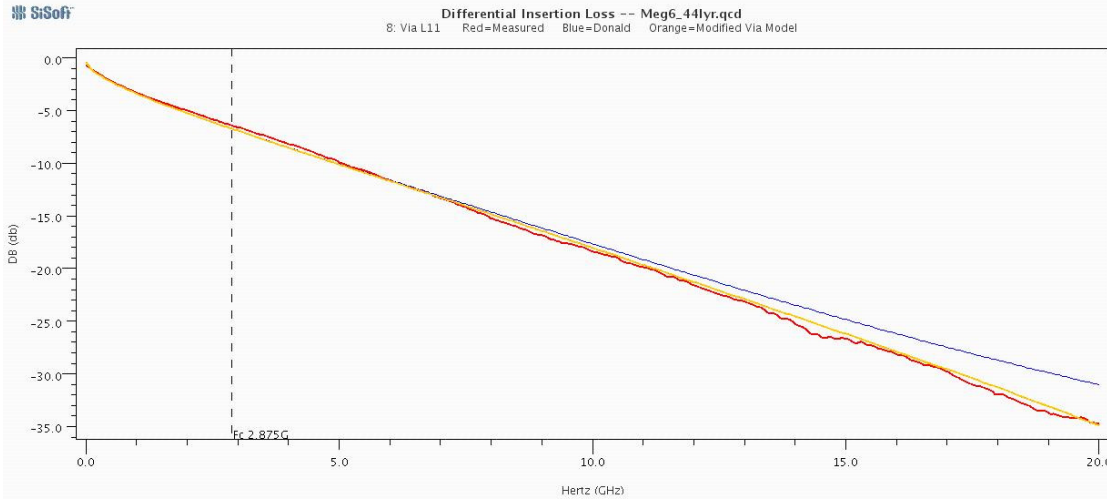


FIGURE 12. Modeled vs. measured insertion loss for 28.3” path length and 0.083” via length

3.2 Stitch Board Data

To further test the excess via loss hypothesis, we applied the same empirical via model (Equation 1, Table 2) to measured data from a via stitch board. This board had been specifically designed to evaluate PC board structures such as vias. For example, one configuration (1.6) contained eight vias while another configuration (4.3) had almost exactly the same length, but only two vias. The material was FR4 rather than the Megtron 6 used in the baseline board, thus requiring a different dielectric constant and dielectric loss tangent. In all other respects, the modeling of the stitch board was exactly the same as the modeling for the baseline data.

TABLE 3. Stitch board configurations

Configuration	Total Length	Vias
1.1	1.34”	2
1.6	11.9”	8
4.1	2.2”	2
4.2	8.1”	2
4.3	12.0”	2

The equipment used to measure the stitch board does not measure the S parameters at low frequency quite as accurately as the the equipment used to measure the baseline data, and this inaccuracy shows up as a baseline shift in the TDR traces calculated from the S parameters.

Also, the bulkhead SMA connectors used on the stitch board start supporting multimode propagation (as opposed to pure TEM mode) at about 14 GHz, making the data above that frequency invalid.

The following figures compare model TDR and insertion loss (RED) to measured results (BLUE) for each of the five stitch board configurations.

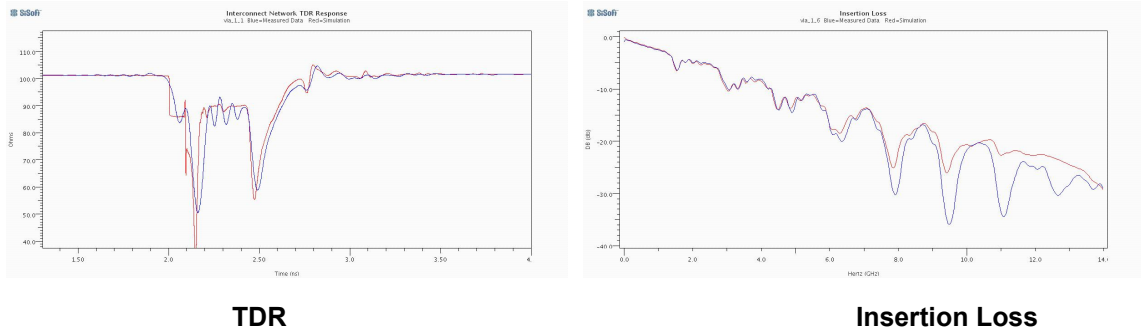


FIGURE 13. Model vs. measurement for stitch board configuration 1.1

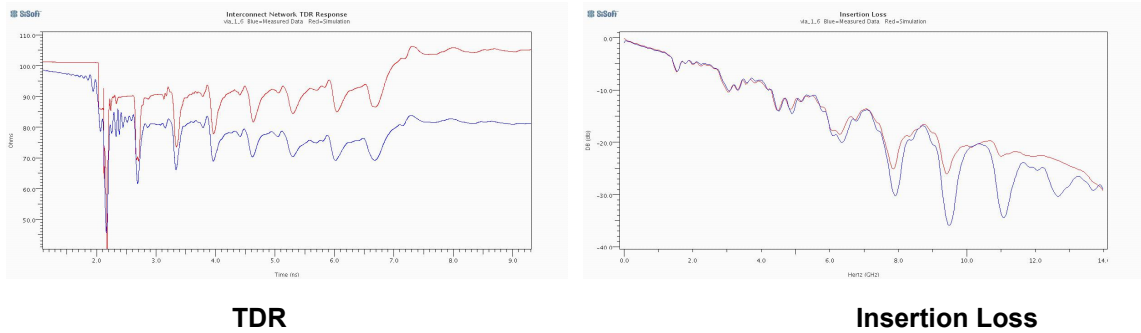


FIGURE 14. Model vs. measurement for stitch board configuration 1.6

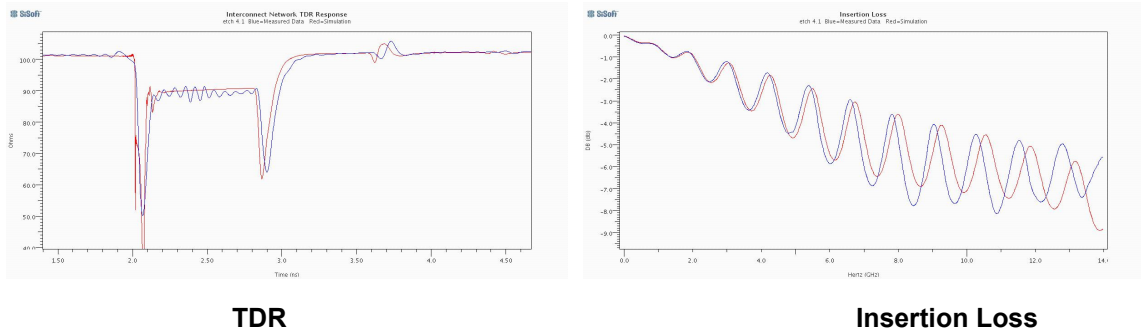


FIGURE 15. Model vs. measurement for stitch board configuration 4.1

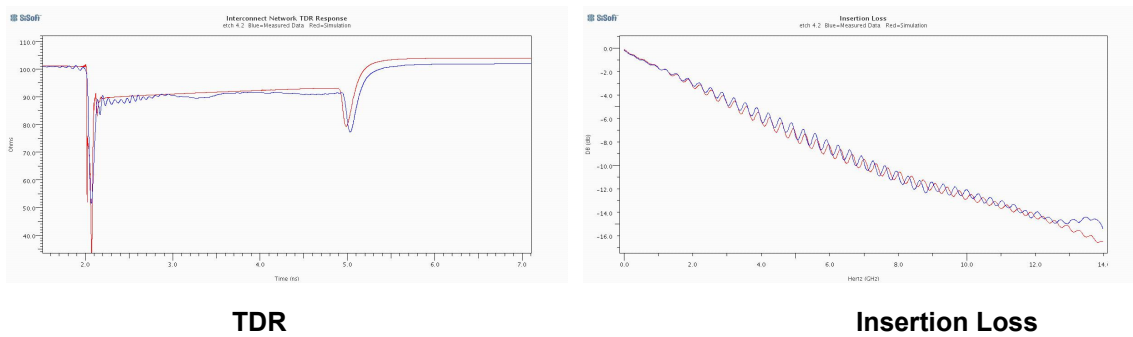


FIGURE 16. Model vs. measurement for stitch board configuration 4.2

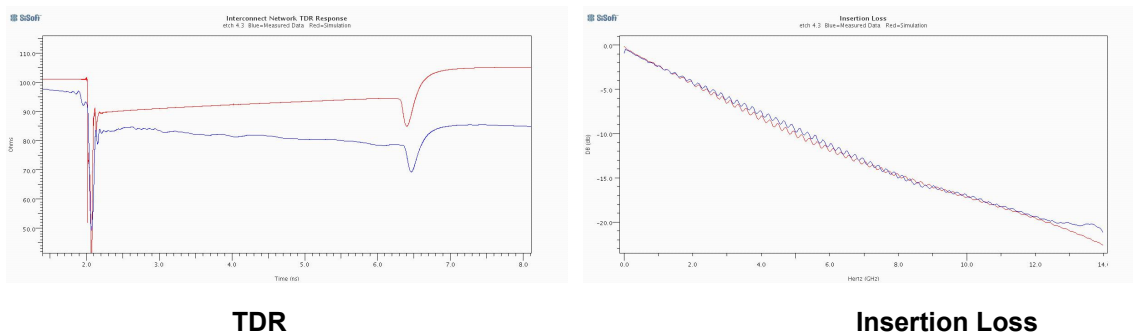


FIGURE 17. Model vs. measurement for stitch board configuration 4.3

As was the case with the baseline data, the results obtained using the empirical model are very encouraging, and particularly the fact that good correlation was obtained for approximately the same trace length (12”) and two very different numbers of vias (8 for configuration 1.6, Figure 14, vs. 2 for configuration 4.3, Figure 17).

3.3 Empirical Model Conclusion

Results obtained using the empirical model for both the baseline data and the stitch board consistently support the hypothesis that vias produce direct, resistive loss at high frequencies in addition to the reflective losses they produce through impedance discontinuities. The support for this hypothesis appears to be strong enough to warrant a theoretical study into the Physics of possible loss mechanisms.

4.0 Electromagnetic Description

This section attempts to gain further insight into via loss by examining the electromagnetic modes associated with vias. Three separate sets of modes are considered: the electromagnetic modes associated with common mode electrical excitation, the electromagnetic modes associated with differential mode electrical excitation, and the electromagnetic modes associated with the transition from vias to stripline transmission lines.

The discussion of common mode excitation is intended to provide a link back to earlier work [1], and to establish a context for the discussion of differential mode excitation. The treatment of differential excitation is the primary concern of this paper. The discussion of the via to trace transition is more complex than can be presented in this paper, and the discussion is therefore qualitative rather than quantitative.

For the common mode and differential mode excitations, the approach is to use magnetic contours to determine the current driven into the various electromagnetic modes. Losses will then be calculated for the electromagnetic modes. It will be seen that although in common mode, all current must be returned through the ground path, in differential mode the currents in the ground path are a function of the via design. Therefore, whereas the losses in common mode can only be avoided through the use of ground vias, the losses in differential mode can be reduced by the use of racetrack-type antipads as well.

4.1 Radial TEM Waves

As demonstrated in [1], the fields associated with a via antipad can be described using radial TEM modes. The electric field for these modes is perpendicular to the ground planes and thus develops a voltage between the ground planes. The dominant magnetic fields for the common and differential modes are illustrated in Figure 18. The magnetic fields exist between the ground planes and are parallel to them. Note that for the differential mode, the magnetic fields rotate in opposite directions around the two signal conductors because the current is flowing in opposite directions in the two conductors.

The corresponding currents flowing in the ground planes and perpendicular to the magnetic fields are illustrated in Figure 19.

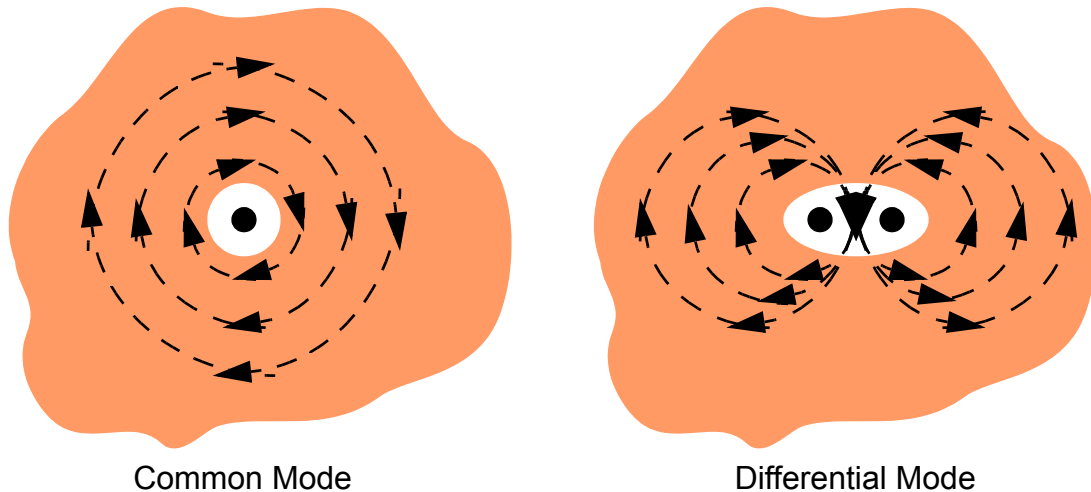


FIGURE 18. Radial TEM mode magnetic fields

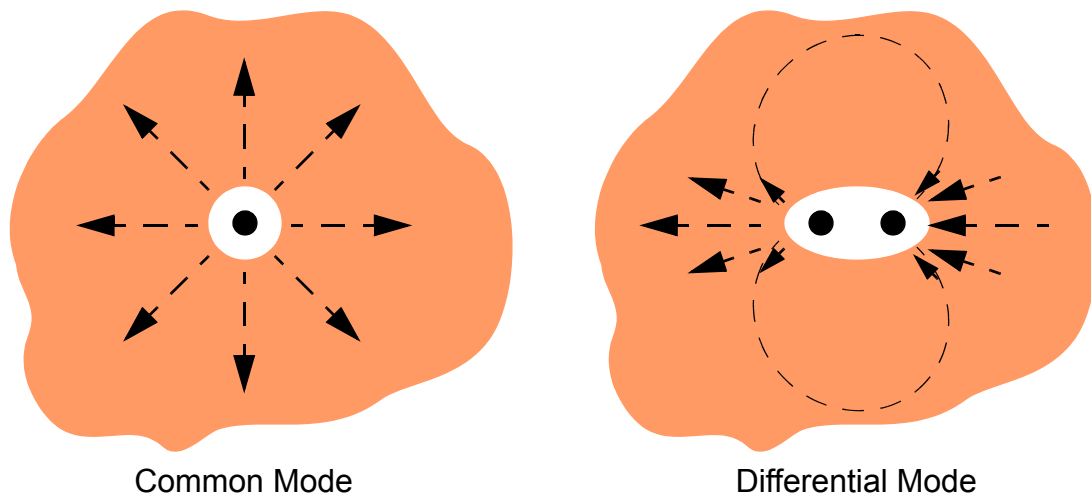


FIGURE 19. Radial TEM mode currents

While the discussion below treats the common mode and differential mode electromagnetic fields in the most detail, other, higher order modes can exist, and are important in the transition from via to trace. While the common mode has no circumferential variation and the differential mode varies through one full cycle in one circle around the via, and is therefore called the first circumferential mode. The higher modes can vary by any integer number of cycles in one circle around the via.

4.2 Common Mode

This section presents an analysis of the insertion loss of a via when driven in common mode. This provides a link back to earlier work [1] and establishes a format which will then be used to analyze the insertion loss of a via in differential mode.

The analysis of common mode starts with the recognition that the current flowing around the edges of the antipad is equal and opposite to the current flowing in the via barrel. Figure 20 shows a magnetic contour defined to be entirely in the metal of a ground plane. Assuming that the metal is more than a few skin depths thick, the magnetic field along this contour is zero. Therefore, the integral of all the current crossing the contour is zero. Since current can cross the contour by flowing along the via barrel, there has to be another current path for an equal and opposite return current. This path is along the edges of the antipad.

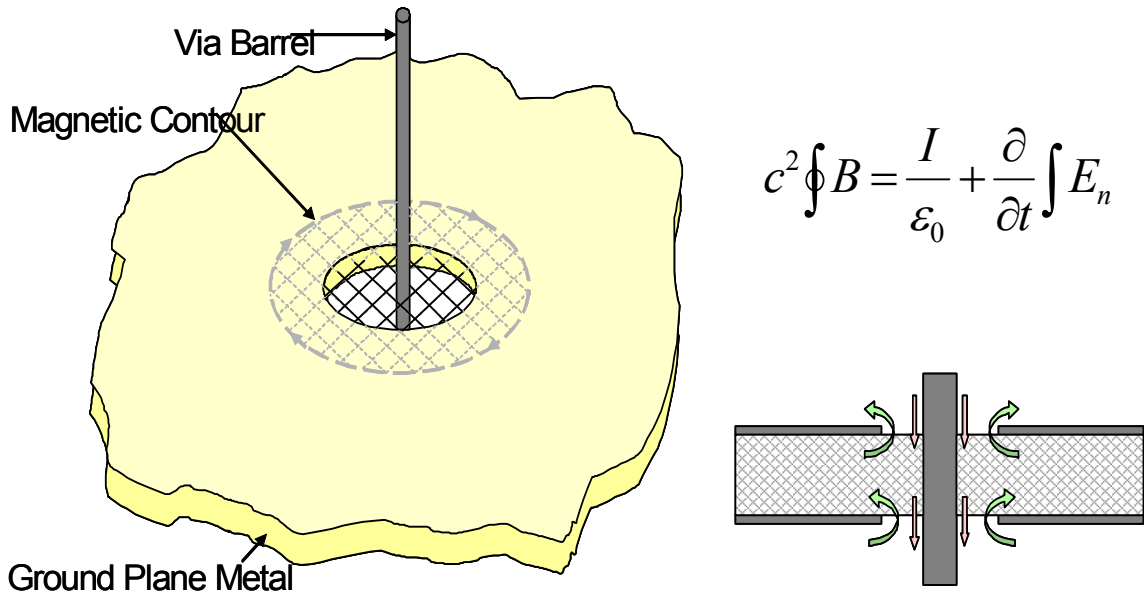


FIGURE 20. Fundamental via current theorem

The current flowing across the edges of the antipad generate radial TEM waves between the ground planes. Although in general there can be both outgoing and incoming waves, this analysis will assume that the incoming waves are negligible. The equations for these waves as a function of radius r are

$$E_z = A(J_0(kr) - jN_0(kr)) \quad (\text{EQ 2})$$

$$H_\phi = \frac{j}{\sqrt{\frac{\mu}{\epsilon}}} A(J_1(kr) - jN_1(kr)) \quad (\text{EQ 3})$$

where

$$k = \omega \sqrt{\mu \epsilon} = \frac{2\pi}{\lambda} \quad (\text{EQ 4})$$

Given dielectric thickness d , the impedance presented at the edge of the antipad is

$$Z_{total} = \frac{-d E_z}{2\pi r H_\phi} \quad (\text{EQ 5})$$

This is an impedance inserted into the ground current return path, and introduces both an impedance discontinuity and an insertion loss. Combining Equation 2 through Equation 5 gives

$$Z_{total} = \frac{jd}{2\pi r} \sqrt{\frac{J_0(kr) - jN_0(kr)}{\epsilon J_1(kr) - jN_1(kr)}} \quad (\text{EQ 6})$$

Figure 21 shows the real and imaginary parts of the antipad common mode impedance for an antipad diameter of 0.04”, a dielectric thickness of 0.1” and a dielectric constant of 3.4.

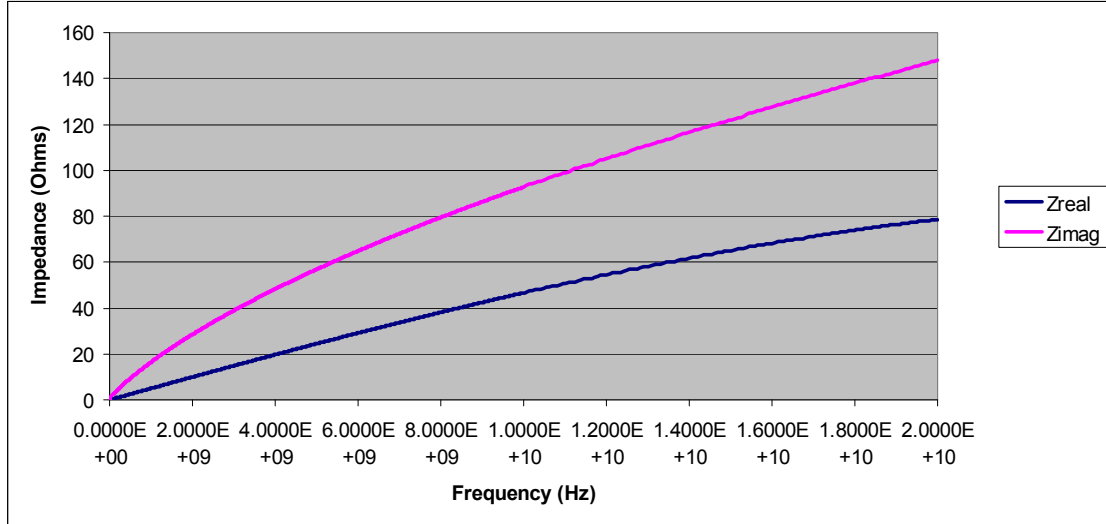


FIGURE 21. Antipad common mode impedance for a 0.04” antipad diameter, 0.1” board thickness and dielectric constant of 3.4

It is interesting to note in Figure 21 that the common mode ground impedance is a linear function of frequency, and that it would introduce an insertion loss of 2.7 dB in a 50Ω path. As described in [1], the insertion loss will be much lower if there are ground vias within a quarter wavelength radius of the signal via.

4.3 Differential Mode

For differential mode, the voltage at the edge of the antipad is not constant. Therefore one cannot define a single impedance for the ground current path the way we did in the previous section for common mode. Instead, we must calculate the current and voltage at the edge of the antipad as a function of angle and then estimate the loss due to ground currents by integrating over that angle. Dividing by the square of the signal current will then produce an equivalent loss resistance, in the sense that the loss is the same as if the signal current had passed directly through a resistor with that value.

Figure 22 illustrates the magnetic contour for analyzing differential mode. In this case, the contour only surrounds one of the two signal conductors, and it does not lie entirely inside the ground plane metal. Instead, there is a segment of the contour that crosses the antipad between the two signal conductors.

Because the currents in the signal conductors have equal magnitude but opposite sign, the magnetic fields they generate add constructively along that portion of the magnetic contour that crosses the antipad. Thus, there is a net current flowing through the surface of the contour, and the currents at the edge of the antipad do not completely offset the currents in the signal conductor. Therefore, the magnitude of the first circumferential TEM mode is smaller, reducing the losses suffered by the differential mode transmission.

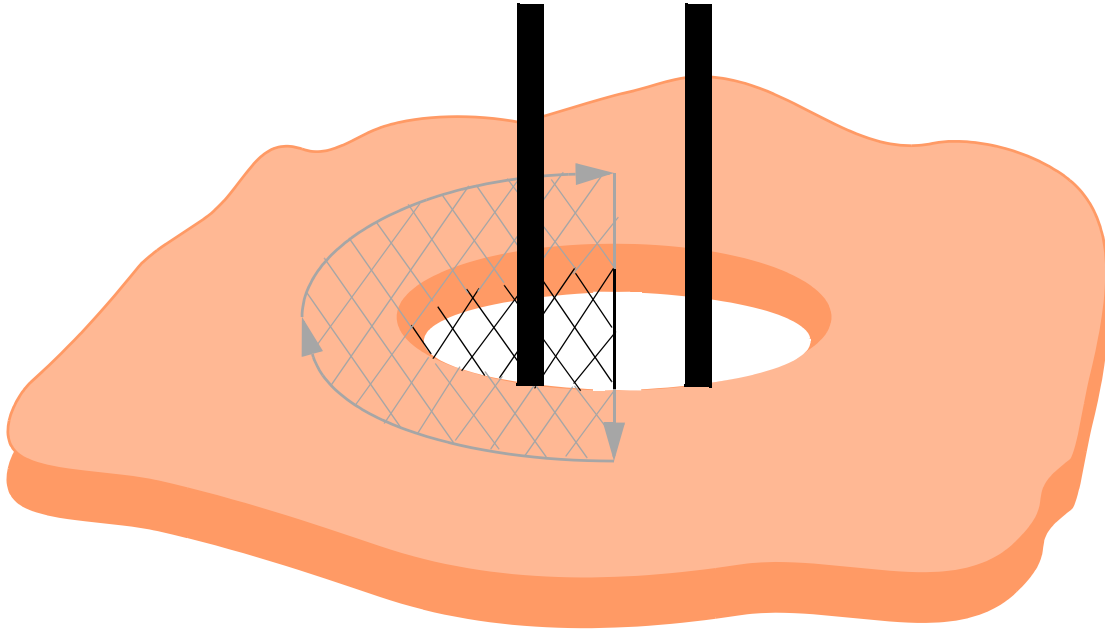


FIGURE 22. Magnetic contour for differential mode

To calculate the total amount of current penetrating the magnetic contour, we will focus our attention on that portion of the contour that crosses the antipad. Given signal conductor current I_s , the magnetic field at a radius r from one signal conductor is

$$H_\phi = \frac{I_s}{2\pi r} \quad (\text{EQ 7})$$

Supposing that the signal conductors are separated by a distance s , and recognizing that the magnetic field varies as one over the distance from the signal conductor, the magnitude of the magnetic field at a distance x from the center of the contour section crossing

the antipad is $\frac{I_s}{2\pi \sqrt{\left(\frac{s}{2}\right)^2 + x^2}}$ of which the fraction which is parallel to the contour line is

$\frac{s}{2\sqrt{\left(\frac{s}{2}\right)^2 + x^2}}$. Define the height of the antipad (length of the contour line crossing the antipad) as b . Then to calculate the ground path current I_g and accounting for the magnetic fields from both signal conductors, the integral of the magnetic field along the contour line from one antipad is

$$\begin{aligned}
 I_s - I_g &= \int_{-\frac{b}{2}}^{\frac{b}{2}} \frac{2I_s}{2\pi\sqrt{\left(\frac{s}{2}\right)^2 + x^2}} \frac{s}{2\sqrt{\left(\frac{s}{2}\right)^2 + x^2}} dx \\
 &= \frac{I_s}{\pi} \int_{-\frac{b}{2}}^{\frac{b}{2}} \frac{\frac{s}{2}}{\left(\frac{s}{2}\right)^2 + x^2} dx \\
 &= \frac{I_s}{\pi} \int_{-\frac{b}{2}}^{\frac{b}{2}} \frac{1}{1 + \left(\frac{2x}{s}\right)^2} d\frac{2x}{s} \\
 &= 2\frac{I_s}{\pi} \operatorname{atan}\left(\frac{b}{s}\right)
 \end{aligned} \tag{EQ 8}$$

Therefore, the ground current on one half of the antipad when driven by a differential signal is

$$I_g = I_s \left(1 - \frac{2}{\pi} \operatorname{atan}\left(\frac{b}{s}\right)\right) \tag{EQ 9}$$

For example, if the antipad height is equal to the signal conductor spacing, then the ground path current will be exactly half the signal conductor current. Conversely, if there is ground metal separating the two signal conductors, then the ground current will exactly equal the signal conductor current.

This equation has direct practical implications in that it implies that the losses of vias in differential mode can be minimized by using racetrack shaped antipads and keeping the via barrels as close together as practical.

Knowing the current in the first circumferential radial TEM mode, we can calculate its effective impedance and therefore the losses introduced to differential mode transmission. From [12], and substituting derivatives of Bessel functions as needed, the pertinent fields are

$$E_z = A(J_1(kr) - jN_1(kr)) \sin(\phi) \tag{EQ 10}$$

$$H_\phi = \frac{j}{\sqrt{\frac{\mu}{\varepsilon}}} A \left(\left(J_0(kr) - \frac{1}{kr} J_1(kr) \right) - j \left(N_0(kr) - \frac{1}{kr} N_1(kr) \right) \right) \sin(\phi) \quad (\text{EQ 11})$$

The current flowing on one side of the first circumferential mode is found by integrating Equation 11 from 0 to pi.

$$I_g = 2A \frac{j}{\sqrt{\frac{\mu}{\varepsilon}}} \left(\left(J_0(kr) - \frac{1}{kr} J_1(kr) \right) - j \left(N_0(kr) - \frac{1}{kr} N_1(kr) \right) \right) \quad (\text{EQ 12})$$

Combining Equation 9 and Equation 12, we get an equation for the amplitude of the fields in terms of the signal current

$$A = \frac{I_s \left(1 - \frac{2}{\pi} \text{atan} \left(\frac{b}{s} \right) \right) \sqrt{\frac{\mu}{\varepsilon}}}{2j \left(\left(J_0(kr) - \frac{1}{kr} J_1(kr) \right) - j \left(N_0(kr) - \frac{1}{kr} N_1(kr) \right) \right)} \quad (\text{EQ 13})$$

Recognizing that the voltage is the layer thickness times E_z , the energy flow for each angle (integral of Poynting's vector across the dielectric thickness) is

$$P(\phi) = -dE_z(\phi)H_\phi(\Phi) \quad (\text{EQ 14})$$

The equivalent ground resistance for one of the two signal conductors is then obtained by integrating over the angle ϕ from 0 to pi and dividing by the mean square of the signal conductor current. The result, comparable to Equation 6, is

$$Z_g = j\frac{\pi}{4} \left(1 - \frac{2}{\pi} \text{atan} \left(\frac{b}{s} \right) \right)^2 d \sqrt{\frac{\mu}{\varepsilon}} \frac{J_1(kr) - jN_1(kr)}{\left(J_0(kr) - \frac{1}{kr} J_1(kr) \right) - j \left(N_0(kr) - \frac{1}{kr} N_1(kr) \right)} \quad (\text{EQ 15})$$

Figure 23 is an example calculation of the equivalent ground resistance for a 0.04" antipad diameter, 0.08" via barrel separation, 0.1" board thickness and dielectric constant of 3.4. This resistance would result in an insertion loss of 0.4 dB at 20 GHz, which is perhaps a quarter of the value predicted by the measured data. Also, the computed ground resistance does not increase as rapidly with frequency as the measured data suggests. As was the case with the common mode calculations, ground vias may significantly reduce the insertion loss at lower frequencies, but will be more than a quarter wavelength away at the higher frequencies. More study is needed in this area.

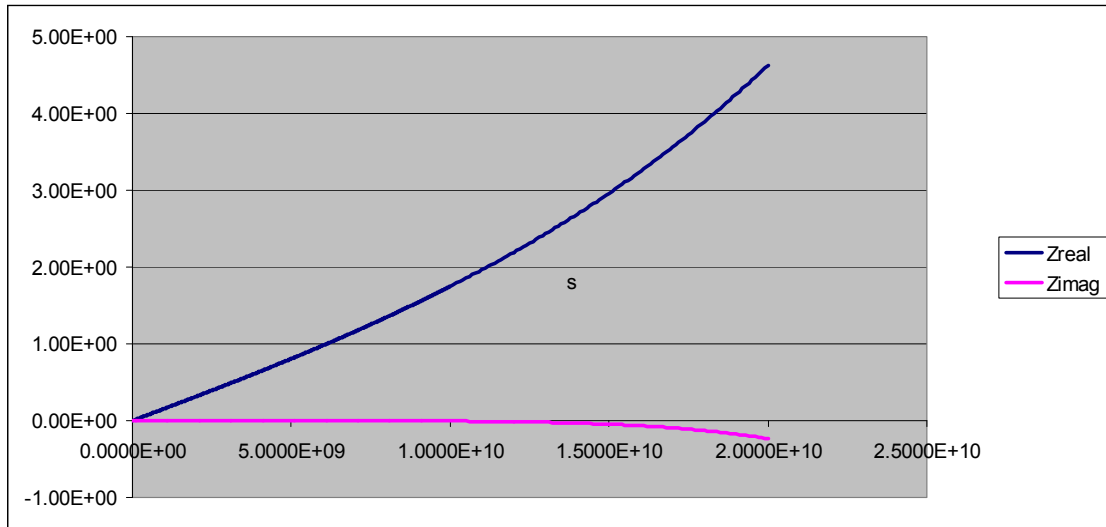


FIGURE 23. Equivalent ground impedance for a 0.04” antipad diameter, 0.08” via barrel separation, 0.1” board thickness and dielectric constant of 3.4

4.4 Transition from Via to Trace

Whenever a via connects to a signal trace, the ground currents associated with signal propagation in the via must somehow find their way to the regions of the ground planes above and below the signal trace. In particular, the current must be continuous at the edge of the antipad, where the radial TEM waves of the via barrel meet the TEM waves from the signal trace.

In the case of differential vias and differential traces, this process can become even more complex because even if the odd mode impedances of the via and signal trace happen to be equal, making their differential impedances equal, their even mode impedances need not be equal. Thus, additional ground currents could be induced at the interface.

Archambeau et. al. [13] have demonstrated that at least for a via through a single ground plane and attached to traces on both sides, the angle between the entry and exit traces can significantly affect the insertion loss at 15 GHz and higher frequencies. This suggests that the current could become crowded toward the side of the via where the trace enters or exits.

All of this reasoning suggests that there will be higher circumferential mode radial TEM waves at the interface between a via and a signal trace, and that these higher order modes will concentrate the current in the direction of the signal trace. By concentrating the current, these higher order modes will also increase the impedance and loss of the via in that region. This is all consistent with our measured data, in that the measured data indicates that shorter vias have higher impedance and higher loss per unit length than predicted by a transmission line model of the via barrel.

Our measured data also indicates, however, that for longer vias, the impedance does match that predicted by a transmission line model of the via barrel. We therefore hypothesize that the higher order circumferential modes exist in the ground plane layers near the signal trace, but that they somehow decay for ground plane layers further from that interface. For every radial TEM mode, however, the currents at the top of the ground plane layer are exactly opposite to those at the bottom of the layer; suggesting that the radial TEM modes should be exactly the same for every ground plane layer a via barrel passes through. So we currently have no physical description for how this decay of higher order modes could occur.

5.0 Conclusions

This paper has demonstrated that discrepancies between the modeled and measured insertion loss of electrical interconnects at high frequencies could be due to dissipative losses in vias due to the generation and subsequent dissipation of radial TEM waves by the via ground return currents.

Analysis of the magnetic fields in the via suggests that for differential vias driven in differential mode, these losses can be minimized by using racetrack shaped antipads and bringing the via barrels in the differential via as close together as practical.

There are a number of areas for future study:

1. Although Section 4.3 on page 19 offers equations for via differential mode insertion loss based on physical modeling, we have not yet correlated results from these equations to measured data.
2. Interactions with ground vias will affect the insertion loss, especially if they are within a quarter wavelength of the signal via. However, especially for differential mode, these interactions will depend on the exact placement of the ground vias, and the effect could be complex.
3. We have hypothesized that higher order circumferential radial TEM waves generated at the interface to signal traces increases the impedance of the via barrel near that interface, but that these modes decay for ground plane layers further away from that interface. This hypothesis has not been tested.

6.0 References

1. Chong Ding, Divya Gopinath, Steve Scarce, Mike Steinberger, Doug White, "A Simple Via Experiment", paper 5-TP2, DesignCon2009, February 3, 2009.
2. Donald Telian, Sergio Camerlo, Brian Kirk, "Simulation Techniques for 6+ Gbps Serial Links", DesignCon 2010, February 2010.
3. Mike Steinberger, Paul Wildes, Mike Higgins, Eric Brock, Walter Katz, "When Shorter Isn't Better", DesignCon 2010, February 4, 2010.

4. Donald Telian, Sergio Camerlo, Michael Steinberger, Barry Katz, Walter Katz, “Simulating Large Systems with Thousands of Serial Links”, paper 8-WA3, DesignCon 2012, February 2012.
5. Mike Steinberger, “TDR: Reading the Tea Leaves”, EEWeb online magazine, http://www.eeweb.com/blog/michael_steinberger/tdr-reading-the-tea-leaves, June 14, 2012.
6. Djordjevic, Biljic, Likar-Smiljanic and Sarkar, “Wideband Frequency-Domain Characterization of FR-4 and Time-Domain Causality”, IEEE Transactions on Electromagnetic Compatibility, Vol. 43, No. 4, pg. 662-7, November 2001.
7. Brist, Hall, Clouser and Liang, “Non-Classical Conductor Losses due to Copper Foil Roughness and Treatment”, presented in the ECWC 10 Conference at IPC Printed Circuits Expo^R, SMCMA Council APEX^R and Designer’s Summit 05.
8. Dai Fen, Mike Harwood, Huang Chunxing, Mike Steinberger, “A Tale of Long Tails”, DesignCon 2010, February 4, 2010.
9. Feynman, Leighton and Sands, *The Feynman Lectures on Physics*, vol II, ch. 32, Addison Wesley, copyright 1964.
10. Ramo, Whinnery and Van Duzer, *Fields and Waves in Communication Electronics*, third edition, section 4.5, John Wiley and Sons, Inc, copyright 1994.
11. Howard Johnson and Martin Graham, *High-Speed Signal Propagation, Advanced Black Magic*, Prentice Hall, pg 71-2, copyright 2003.
12. Ramo, Whinnery and Van Duzer, *Fields and Waves in Communication Electronics*, third edition, sections 7.13, 9.3 and 9.4, John Wiley and Sons, Inc, copyright 1994.
13. Archambeau, Connor, de Araujo, Hashemi, Mittra, Schuster, and Ruehli, “Full Wave Simulation and Validation of a Simple Via Structure”, paper 11-TA1, DesignCon 2006, February 2006.